

## Hand arm vibration measurement using micro-accelerometer in different brick structures

K. Gomathi<sup>\*1</sup>, A. Senthilkumar<sup>2a</sup>, S. Shankar<sup>1b</sup>, S. Thangavel<sup>1c</sup> and R. Mohana priya<sup>1d</sup>

<sup>1</sup>Department of Mechatronics Engineering, Kongu Engineering College, Erode, Tamilnadu, India

<sup>2</sup>Department of Electrical and Electronics Engineering, Dr.MCET, Pollachi, Tamilnadu, India

(Received December 11, 2013, Revised March 25, 2014, Accepted April 10, 2014)

**Abstract.** Hand-Arm Vibration Syndrome (HAVS) is a group of diseases caused by exposure of the hands to vibration while operating the hand held power tools such as road breaker, drilling machine, demolition hammer in construction works. In this paper, area-changed capacitive micro-accelerometer is designed to measure the vibration exposure on worker's hand when operating a drilling machine on various blocks such as clay block, paver block and solid cement block. The design process includes mathematical modelling of micro-accelerometer and simulations are done using INTELLISUITE 8.6. Experimental results are taken for various blocks surfaces using conventional and micro-accelerometer. Comparisons show that usage of area-changed micro-accelerometer for Hand-arm vibration monitoring provides better sensitivity, which in turn reduces the risk of HAVS in workers.

**Keywords:** accelerometer; hand arm vibration; area-changed capacitive type; drilling

### 1. Introduction

Hand arm vibration is experienced at workplace when vibrations from machinery are transferred to the corresponding operators. Excessive exposure to such vibration gives rise to serious health concerns such as numbness and tingling, reduced sensitivity, grip in the hands and white finger syndrome as shown in Fig. 1. Hence, several ISO standards have been laid down to enforce upper limits on the amount of vibration received by workers. The ISO 10819:2013 specifies that vibration transmissible in terms of vibration transmitted from a handle through a glove to the palm of the hand is one third octave frequency bands with centre frequency of 25 to 1250 Hz, while the ISO 15694:2004 specifies methods for measuring single shocks at the handle of hand held and hand guided machinery characterised by maximum strike rate of below 5 Hz. Several researchers have developed novel ideas to measure this vibration in civil structures, so that

---

\*Corresponding author, Ph. D. scholar, E-mail: [gomu\\_k@yahoo.com](mailto:gomu_k@yahoo.com)

<sup>a</sup> Ph. D., E-mail: [asenthil@drmcet.ac.in](mailto:asenthil@drmcet.ac.in)

<sup>b</sup> Ph. D., E-mail: [shankariitm@gmail.com](mailto:shankariitm@gmail.com)

<sup>c</sup> PG Scholar, E-mail: [thangavels.12mmts@kongu.edu](mailto:thangavels.12mmts@kongu.edu)

<sup>d</sup> PG Scholar, E-mail: [mohanaa89@gmail.com](mailto:mohanaa89@gmail.com)

the effects of vibration can be mitigated. Ni *et al.* (2011) developed a wireless structural health monitoring system to protect the super tall structures against vibration effects during construction. Guo *et al.* (2012) proposed a mobile sensor network where each sensor is accompanied by a mobile robot capable of processing vibration data was implemented as a next step towards structural health monitoring of civil structures. Myung *et al.* (2011) developed a multiple paired structured light system to directly calculate the displacement values arising due to vibration in civil structures. Myung *et al.* (2009) used a multiple dual laser vision system to calculate the displacement of structures due to vibration at times of natural calamities like earth quake, and other phenomena like traffic, gust and waves.

A detailed review on vibration-based robust detection techniques is presented by Li and Chen (2013). Currently, a system comprising of conventional accelerometer as the principle component is being utilised to measure this hand arm vibration and protect the workers. But the system is piggy packed with several shortcomings. MEMS based accelerometer serves as a promising alternative over conventional technologies. This technology however took shape only towards the end of twentieth century. Since then, there have been several iterations of this device with significant modifications in the design at each stage. The most recent one amongst these is a capacitive area changing MEMS accelerometer which includes the properties like the exhibition of superior performance in the low frequency range combined with linearity, low noise performance and high sensitivity. Wen *et al.* (2011) fabricated MEMS capacitive accelerometers using low thermal budget SiGe fabrication process. A Printed Circuit Board and Laser ablation based fabrication of MEMS Single axis accelerometer was manufactured by Luque *et al.* (2013). Benmessaoud and Nasreddine (2013) presented an optimization technique to design an MEMS accelerometer to improve its performance. The present paper aims at utilising this accelerometer to measure the hand arm vibrations experienced by workers and warn them when breaching the nominal values specified by ISO standards. In this work, MEMS capacitive area changing accelerometer is designed and developed to measure the vibration experienced by workers while drilling different types of blocks. The same experimentation is carried out with conventional accelerometer to outline the advantages and disadvantages of the two techniques.



Fig. 1 White finger syndrome

## 2. Design and analysis

### 2.1 Mathematical modelling

Accelerometer can be dynamically modelled as a simple mass-spring-damper system. When the accelerometer is excited along the sense direction with acceleration ‘a’, the proof mass ‘m’, suspended by a beam or spring is displaced under the effect of inertial force in a direction opposite to the applied acceleration. The basic equation of a mass-spring-damper system shown in Fig. 2 is

$$M \frac{d^2x}{dt^2} + D \frac{dx}{dt} + Kx = f \tag{1}$$

Where ‘M’ is the mass of the proof mass, ‘D’ is the damping coefficient of the system, ‘K’ is the beam or spring stiffness, ‘a’ is the acceleration along sense direction and ‘x’ is the displacement of the ‘proof mass’.

Since the microaccelerometer is enclosed in a closed package, it resembles like a free vibration system with air as damping medium. Hence the damping co-efficient is considered to be negligible, i.e., D = 0;

Therefore Eq. (1) becomes

$$M \frac{d^2x}{dt^2} + Kx = f = 0 \tag{2}$$

Taking Laplace Transform of Eq. (2), this becomes

$$F(S) = MS^2 X(S) + KX(S) \tag{3}$$

Eq. (3) is rearranged as

$$\frac{X(S)}{F(S)} = \frac{1}{s^2 + \frac{K}{M}} \tag{4}$$

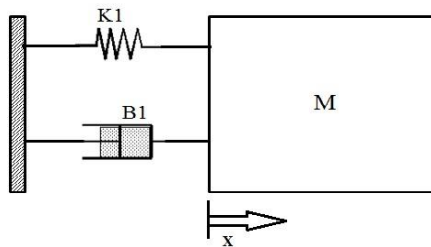


Fig. 2 Mass-Damper-Spring system

To obtain the theoretical results of the proposed micro-accelerometer, three important parameters have to be calculated. They are total mass (m), spring constant (K), and resonant frequency (f) of the system. Total mass of the system is comprised of mass of proof structure and mass of the sensing fingers. This model encompasses 25 sensing fingers

$$m = \rho_{si}(W_p L_p T_p + N W_f L_f T_f) \quad (5)$$

Where  $W_p, L_p, T_p$  are width, length and thickness of proof mass ( $\mu\text{m}$ ),  $W_f, L_f, T_f$  are width, length and thickness of fingers ( $\mu\text{m}$ ), N is the Number of sensing fingers and  $\rho_{si}$  is the mass density of silicon ( $\text{Kg}/\text{m}^3$ ). Using the dimensions from Table.1, the total mass of system is obtained i.e.,  $m = 1.0279\text{e-}7$  Kg. Spring constant of the suspension spring is found by employing Hooke's law of elasticity, which states that for relatively small deformations of an object due to applied load or force, the displacement or size of the deformation is directly proportional to the deforming force or load. Under these conditions the object returns to its original shape and size upon removal of the load. Therefore, Force acting on spring

$$F_{spring} = \bar{n} g - K \Delta t \quad (6)$$

Table 1 Dimensions of the proposed micro-accelerometer

S.No	Parameter	Value ( $\mu\text{m}$ )
1	Length of Proof mass ( $L_p$ )	2360
2	Width of Proof mass ( $W_p$ )	22
3	Thickness of Proof mass ( $T_p$ )	40
4	Length of Finger ( $L_f$ )	2000
5	Width of Finger ( $W_f$ )	20
6	Thickness of Finger ( $T_f$ )	40
7	Length of Spring ( $L_1$ )	560
8	Width of Spring ( $W_1$ )	5
9	Thickness of Spring ( $T_1$ )	40
10	Number of Fingers (N)	25

Where K is the spring constant, Δt is the change in length. Based on the maximum bending stress of the spring, the spring constant (K) Zheng *et al.* (2009) is given by

$$K_x = \frac{N_2 E (2L_1 + \pi R_1) W_1^3 T_1}{2(2L_1^4 + 4\pi R_1 L_1^3 + 24R_1^2 L_1^2 + 6\pi R_1^3 L_1 + 3\pi^2 R_1^4 - 24R_1^4)} \tag{7}$$

Where L<sub>1</sub>, W<sub>1</sub>, T<sub>1</sub> are length, width and thickness of spring (μm), R<sub>1</sub> is the radius of centreline of arc in spring, N<sub>2</sub> is number of springs and E Young’s modulus of material. The spring constant of the suspension spring is found to be K= 9.121 (N/m) for the dimensions tabulated in Table 1. It is much necessary to determine the safe operating frequency of the micro-accelerometer to avoid error’s in measurement values and to prevent system from attaining unstable state. The mechanical resonant frequency ‘f’ can be written as

$$f = \frac{\sqrt{K}}{2\pi} \tag{8}$$

From spring constant (K) and total mass (m), the resonant frequency of the system is theoretically found to be f=1500.038 Hz, which means that designed micro-accelerometer will provide linear results if the impact frequency is lesser than the resonant frequency of 1500 Hz. The dimension of the proposed microaccelerometer model is tabulated in Table 1, the values are collected from the previous researches such as Bais and Majlis (2008), Hsu *et al.* (2008), Zheng *et al.* (2009) .

The fabrication of entire device is done using IntelliFab module in Intellisuite. Mask layer of the microaccelerometer is designed with respect to dimensions specified in Table 1. Process flow to fabricate the microaccelerometer is shown in Fig. 3,

Silicon is chosen to be the base material with orientation of <111>, which possesses high tensile strength. In the second step, the deposition of mask layer over the base silicon substrate was carried out. Third step includes etching of base material with DRIE (Direct Reactive Ion Etching). DRIE provides narrow cut of wall surfaces. Final step is used to clean the etched silicon to remove photoresist used for masking. FabViewer module is used to visualize the fabricated microaccelerometer step by step which is shown in Fig. 4. The final 3D view of the fabricated microaccelerometer is shown in Fig. 5

#	<input checked="" type="checkbox"/>	Type	Material	Process	Process ID	Process Option
1	<input checked="" type="checkbox"/>	Definition	Si	Czochralski	111	
2	<input checked="" type="checkbox"/>	Definition	UV	Contact	Offset	
3	<input checked="" type="checkbox"/>	Etch	Si	Dry	DRIE	Etch Through
4	<input checked="" type="checkbox"/>	Etch	Si	Clean	RCA	

Fig. 3 Process flow

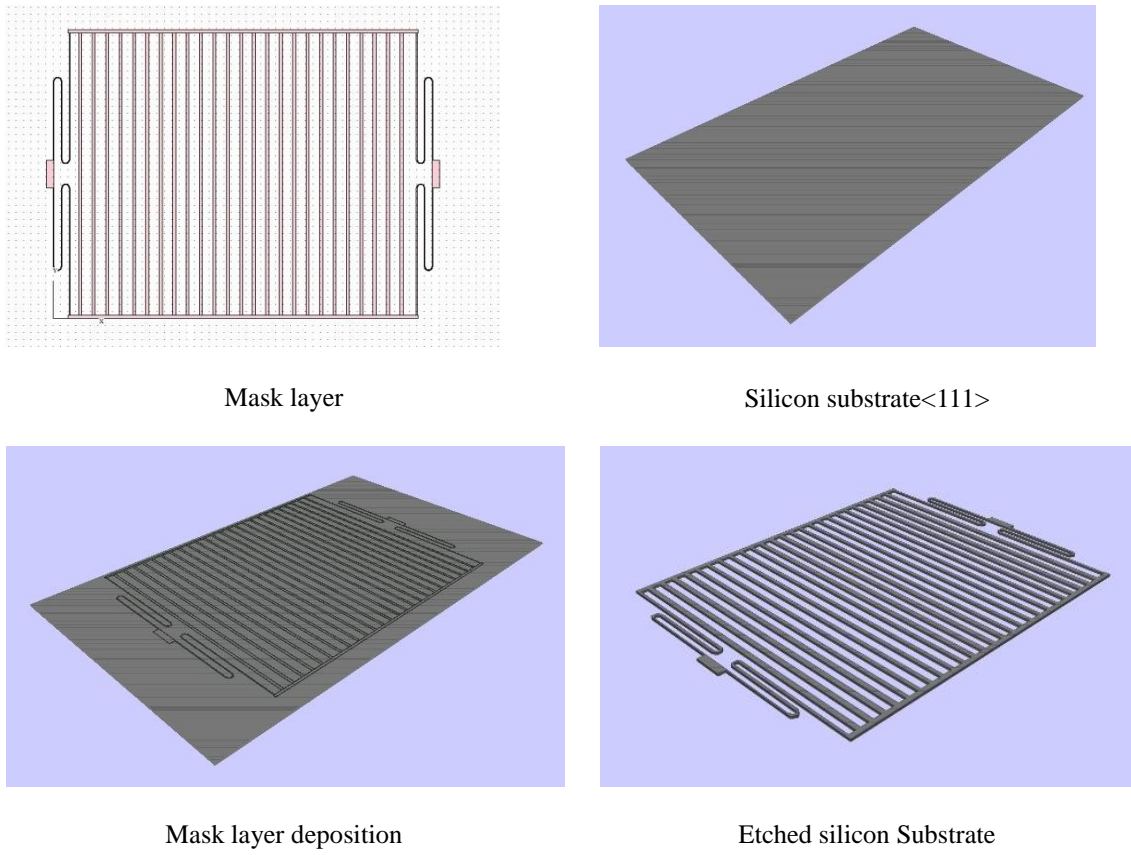


Fig. 4 Fabrication Process sequence in FabViewer

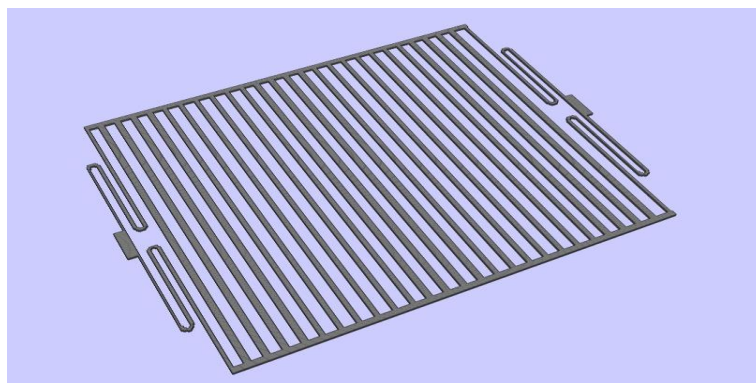


Fig. 5 3D model of micro-accelerometer

Static analysis:

It is a DC analysis procedure where a constant load is applied on a designed device to find its static characteristics. INTELLISUITE is used to perform the analysis for the designed micro accelerometer. The simulation result for the same is shown in Fig. 6.

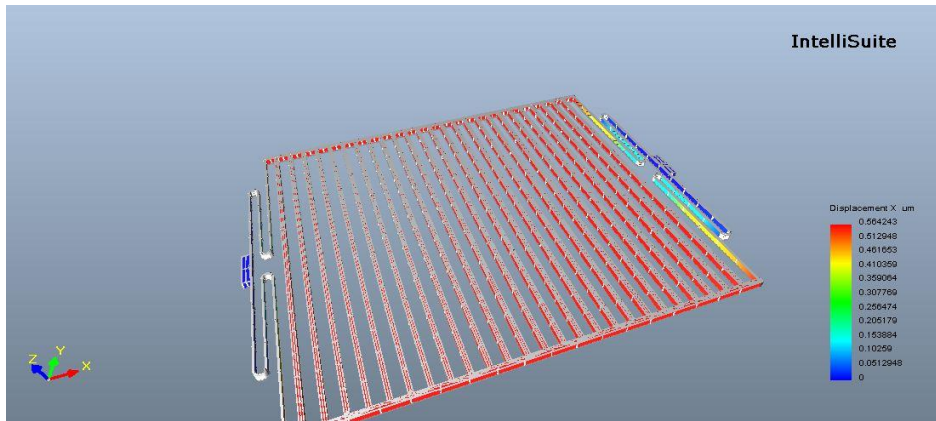


Fig. 6 Displacement along X-axis for applied acceleration load

In order to validate the proposed model it is necessary to analyse the equality of the simulation result which are shown in Fig. 6 with the theoretical result. The applied acceleration is to be 2 g in X-axis. Theoretical displacement (X) in X-axis for 2 g;

$$K = 9.121 \text{ (N/m) or } 9.121e^{-7} \text{ (N/}\mu\text{m)}$$

Total force acting on the system is given by Newton’s 2<sup>nd</sup> law of motion, which states that force developed by a body is directly proportional to product of mass of the body and rate at which it’s accelerating, Total mass of the system  $m=1.0279e^{-7}$  kg, hence total force acting on system,

$$F_{\text{total}} = 1.0279e^{-7} \times 2 \times 9.81 = 2.01673e^{-6} \text{ N} \tag{9}$$

Displacement (X) made by proof mass for the applied acceleration will be

$$X = F_{\text{total}} / K \text{ (}\mu\text{m)} = 0.22110 \text{ (}\mu\text{m)} \tag{10}$$

The simulation results shown in Fig. 6 and calculated theoretical results are compared. The obtained theoretical result matches well with simulation results with minor deviation of 2.03%. Fig. 7 shows the comparison of mathematical and simulated static results with acceleration Vs. displacement along X axis.

Frequency analysis:

This analysis is also called as modal or AC analysis which is used to find out the natural mode shapes and frequencies of a given object or structure during free vibration and also to reduce the noise levels emitted by the accelerometer. It can improve the overall performance of the product in critical working conditions. The analysis is done using INTELLISUITE Thermo Electro Mechanical (TEM) analysis module. The designed micro-accelerometer shown in Fig. 5 is

exported to TEM module and frequency analysis option is chosen in simulation settings. Boundary layers of micro-accelerometer are selected and load voltage of 5V is applied to one side of proof mass. The fixed sensing fingers are given 0V. The simulated results from the analysis are given below:

- Mode 1 - 1487.44 Hz
- Mode 2 - 2599.45 Hz
- Mode 3 - 2731.55 Hz

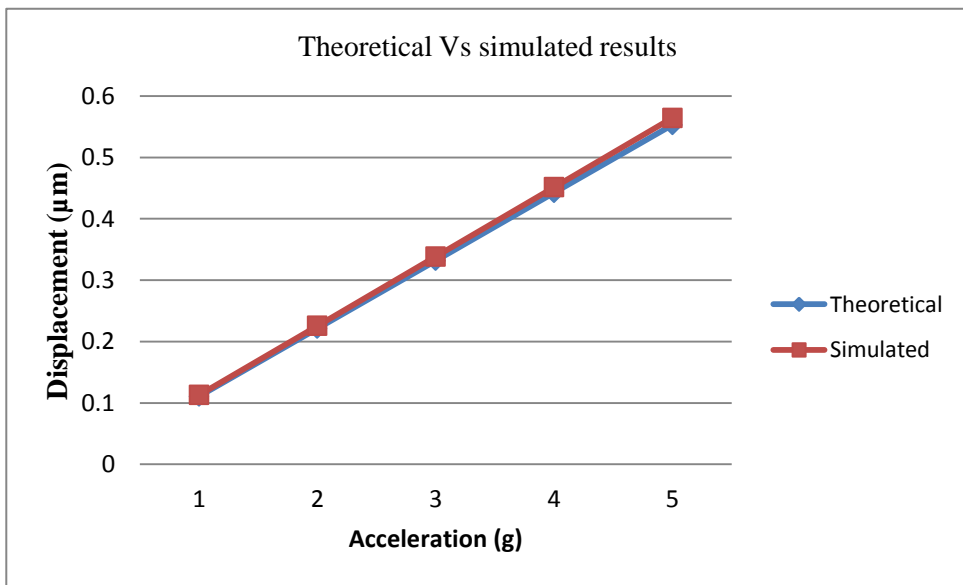


Fig. 7 Comparison between theoretical and simulation static results

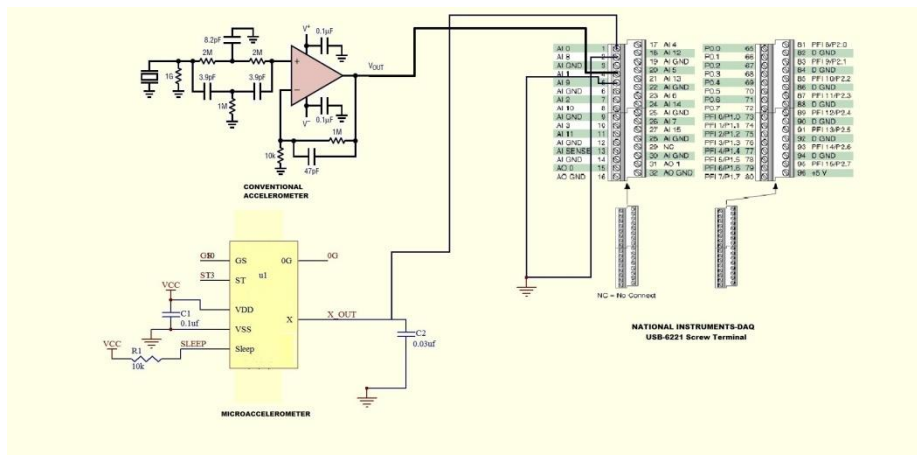


Fig. 8 Interfacing circuit

The Mode 1 operates along X-Axis, Mode 2 and Mode 3 operates along Y-axis and Z-axis. Natural frequency obtained in Mode 1 equal 99.16% to the theoretical value obtained in mathematical modelling which is 1500 Hz. Then the designed accelerometer was fabricated. The sensing circuit for designed microaccelerometer was designed using ORCAD PSPICE software and PCB board layout is designed using the same, which is shown in Fig. 8. The sensitivity of the microaccelerometer was calculated to be 800mV/g with operating range falling between 1g and 30 g. The operating voltage required to operate the microaccelerometer was 2.2-3.6V DC.



(a)



(b)

Fig. 9 (a) Experimental setup and (b) Experimentation using Micro-accelerometer

### 3. Experimental setup

The experimental set up is comprised of conventional accelerometer and microaccelerometer which is designed and fabricated is attached to Hammer drill. The conventional accelerometer is connected to NI USB-6221 DAQ through a signal conditioning unit. Designed microaccelerometer is connected to a signal conditioning unit containing an amplifier and microcontroller, which is shown in Fig. 9(a). In the next step, workers are made to drill the three blocks namely Clay block, paver block, solid cement block and the vibrations produced are recorded by a conventional accelerometer and transduced into a computer via an NI USB- 6221 M series DAQ card which already explained by Xiaohan and Xilin (1996), Lynch *et al.* (2003), Chiu and Moss (2007), Rokkam *et al.* (2007), Peterson *et al.* (2008), Zhang and Chen (2008). NI USB- 6221 is a multifunctional card capable of handling both analog and digital signals. It contain 8 single-ended channel and 4 differential channel with a resolution of 16bits at a sample rate of 250 kS/s. Hammer drill from Robert bosch is used in this experiment, which have impact energy of 5.6 ft/lbs. Entire experimental setup is shown in Fig. 9(b).

The Lab VIEW program used for the interfacing NI USB-6221 DAQ with system to process the acquired data is shown in Fig. 10. DAQ assistant module is used to acquire data from both accelerometers at a sampling rate of 1000S/s. Output from DAQ assistant is given as input to spectral measurement tool to obtain frequency analysis result and also saved as Microsoft Excel document using 'Write to measurement file' tool. To indicate the result during run time of the program, graph indicators CF and CT are used.

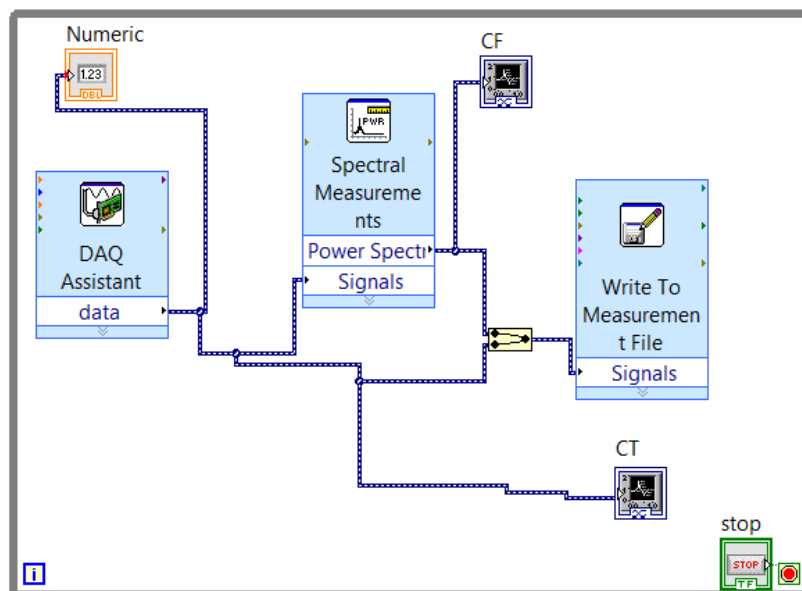


Fig. 10 Lab VIEW design module

### 4. Results and discussions

The readings for different blocks with conventional accelerometer and micro-accelerometer are compared. The results from conventional and micro-accelerometer are compared with applied acceleration required to break the paver block is shown in Fig. 11. The conventional accelerometer produces a maximum of 7.85 g, whereas the micro accelerometer produces a maximum of 6.1 g during the process.

From the obtained results, the EAV and ELV values are calculated using Hand-Arm vibration exposure calculator framed by Health and Safety Executive (HSE) for the acceleration data obtained from both accelerometers. The calculation for these values was done at 21<sup>st</sup> milli second as it exhibits the lowest acceleration value in micro accelerometer and at the same instant the value was measured using conventional accelerometer and the results are tabulated in Table 2. The power absorbed by hand-arm at different frequencies and acceleration value when using the vibrating power tools was elucidated by Dong *et al.* (2005), Dong *et al.* (2006), Dong *et al.* (2008), which shows the importance of working with low acceleration values. This is the reason for choosing the lowest acceleration value, so that to find the additional time for the worker to finish the work assigned to them, without reaching the exposure value. The results shows that micro-accelerometer provide better sensitivity than the conventional accelerometer. A worker operating hammer drill to break a paver block should not cross the EAV time of 44min, which is measured as 49min by conventional accelerometer. The ELV value of 19min exceeds when using the conventional accelerometer, which in turn results serious damage to worker hands.

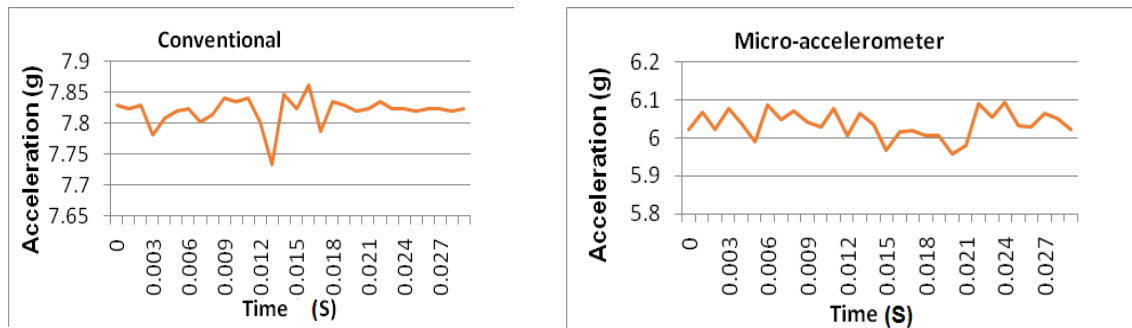


Fig. 11 Comparison of accelerometers result for Paver block

Table 2 EAV and ELV results for 21<sup>st</sup> milli second

BLOCK	TO REACH EAV		TO REACH ELV	
	CONVENTIONAL ACCELEROMETER	MICRO-ACCELEROMETER	CONVENTIONAL ACCELEROMETER	MICRO-ACCELEROMETER
Paver	49min	44min	3hr 14min	2hr 55min

The same procedure is repeated for solid cement block and the obtained results are plotted to exposure time. The results are shown in Fig. 12. The conventional accelerometer produces a maximum of 7.85 g, whereas the micro accelerometer produces a maximum of 6.1 g during the process.

EAV and ELV value are calculated for the lowest acceleration at 21<sup>st</sup> milli second from micro-accelerometer and for the same instant the value measured by conventional accelerometer are tabulated in Table 3. For cement blocks the readings from both accelerometer shows that EAV value from micro-accelerometer is 31min more than conventional, which means that the worker have another 31min to work with cement block demolition process and ELV value of 2hr 5min is extra time for the worker to work under safety condition.

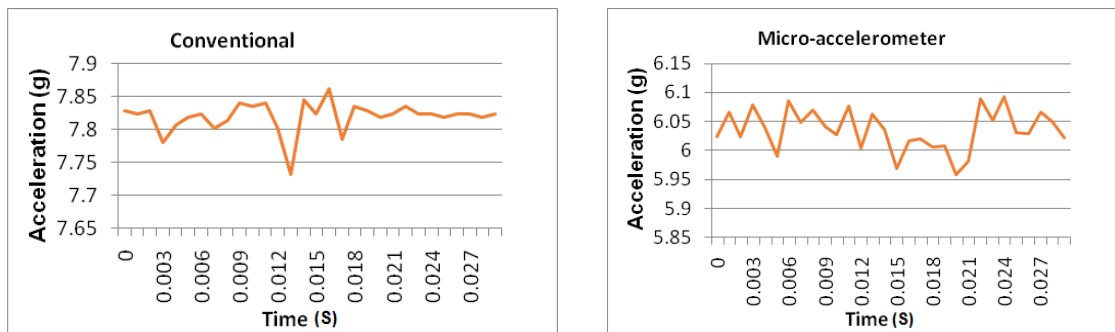


Fig. 12 Comparison of accelerometers result for Solid cement block

Table 3 EAV and ELV result for 21<sup>st</sup> milli second

BLOCK	TO REACH EAV		TO REACH ELV	
	CONVENTIONAL ACCELEROMETER	MICRO-ACCELEROMETER	CONVENTIONAL ACCELEROMETER	MICRO-ACCELEROMETER
Cement Block	47min	1hr 18min	3hr 8min	5hr 13min

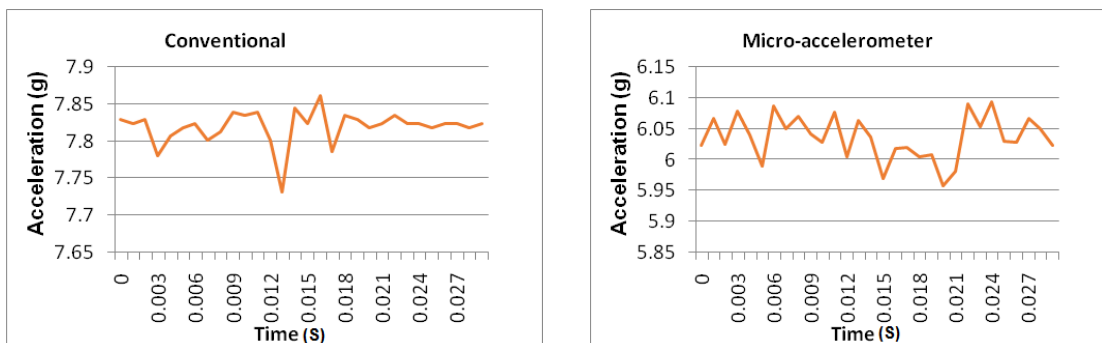
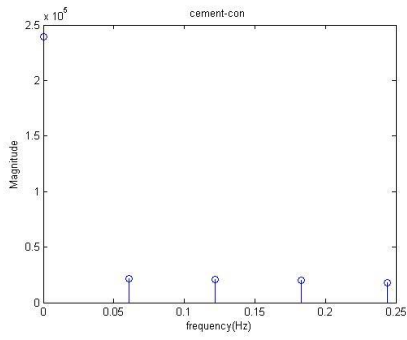
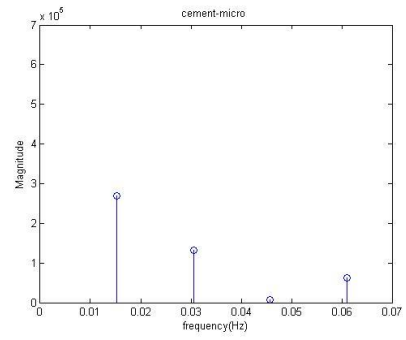


Fig. 13 Comparison of accelerometers reading for Clay block

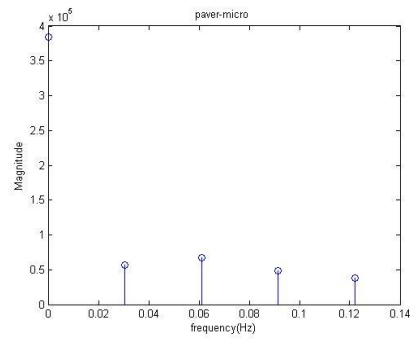
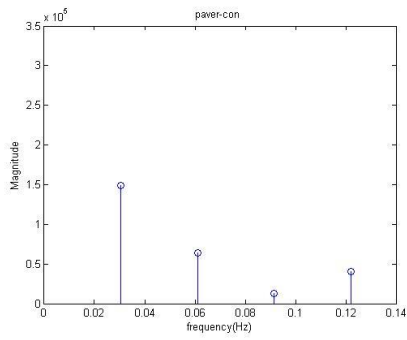
FFT for conventional accelerometer



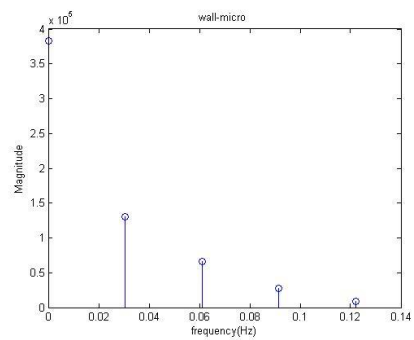
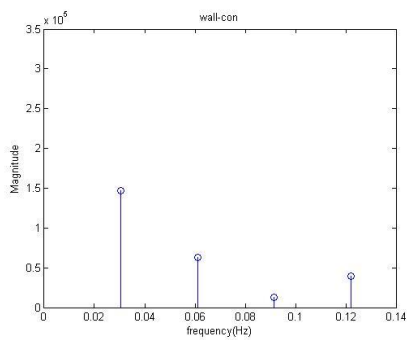
FFT for microaccelerometer



(a) Solid Cement block



(b) Paver block



(c) Clay block

Fig. 14 Vibration spectra in sensing axis for both accelerometers

The results of Clay block demolition process reading are plotted against vibration exposure time and shown in Fig. 13. The conventional accelerometer produces a maximum of 7.85 g, whereas the micro accelerometer produces a maximum of 6.1 g during the process. The EAV and ELV values are calculated for readings of conventional and micro -accelerometer readings and tabulated in Table 4.

EAV value of micro-accelerometer shows that the worker assigned for demolition of Clay block have 1hr 25min to reach exposure active value, and 5hr 38min to reach exposure limit value. These values will allow the worker to finish the work soon without any damage to hands.

The fast fourier transform analysis was done using MATLAB coding was given in Fig. 14. It was found that the maximum vibration occurs within 0 to 0.25 Hz while breaking the three blocks namely Paver, Clay and Cement. This mainly happens in the X axis predominantly. By comparing the results of FFT, the vibration spectra for paver block shows that vibrations in conventional accelerometer has a higher magnitude at 0.03 Hz, whereas for the same vibrations in microaccelerometer, the higher magnitude occurs at 0.06 Hz . Due to peak magnitude occurrence in conventional accelerometer at 0.03 Hz the work time gets reduced. Similarly while using conventional accelerometer for clay block, the work time is reduced. Thus in order to enhance the working time, microaccelerometer has to be used. Thus from the Hand Arm vibration exposure calculator, the precise values for EAV and ELV are calculated using micro-accelerometer. The person working in Clay block takes 1Hours 25minutes to reach EAV and 5Hours 38minutes to reach ELV, person working in paver block takes 44minutes to reach EAV and 2Hours 55minutes to reach ELV and person working in solid cement takes 1Hours 18minutes to reach EAV and 5Hours 13minutes to reach ELV. The comparison of conventional and micro-accelerometer results for paver block shown in Table 2 is more or less equal, as paver block is a softer material. Moreover, the microaccelerometer is more sensitive, due to which the calculation of EAV and ELV values gave precise and accurate results. This would enable the workers to keep a precise cap on their remaining working time. Thereby, risk of getting HAVS could be reduced drastically.

Table 4 EAV and ELV result 21st milli second

BLOCK	TO REACH EAV		TO REACH ELV	
	CONVENTIONAL ACCELEROMETER	MICRO-ACCELEROMETER	CONVENTIONAL ACCELEROMETER	MICRO-ACCELEROMETER
Clay Block	49min	1hr 25min	3hr 16min	5hr 38min

## 5. Conclusions

Thus micro-accelerometer is designed for measuring hand arm vibration using INTELLISUITE 8.6 and fabricated. Then a conventional accelerometer is also used to measure the hand arm vibrations for comparison with the microaccelerometer. The vibrations were transduced with LABVIEW programming via DAQ card (Model: NI USB- 6221) and exact time to reach EAV of 2.5g A(8) and ELV of 5g A(8) by a person working on paver block, solid cement block and clay block on that day is calculated using both accelerometers. The comparison result shows that the worker is getting exact value of time to finish the demolition work without facing any risk when using micro-accelerometer over conventional accelerometer. This is due to higher sensitivity and

accuracy of the fabricated microaccelerometer for Hand-arm vibration measurement. In future, the hand arm vibrations of different persons with various kinds of materials would be measured using the micro-accelerometer to test its versatility.

## References

- Bais, B. and Majlis, B.Y. (2008), "Low-g area-changed MEMS accelerometer using bulk silicon technique", *Am. J. Appl. Sci.*, **5**(6), 626-632.
- Benmessaoud, M. and Nasreddine, M.M. (2013), "Optimization of MEMS capacitive accelerometer", *Microsyst. Technol.*, **19**(5), 713-720.
- Chiu, C. and Moss, C.F. (2007), "The role of the external ear in vertical sound localization in the free flying bat, *Eptesicus fuscus*", *J. Acoust. Soc. Am.*, **121**(4), 2227.
- Dong, J.H., Dong, R.G., Rakheja, S., Welcome, D.E., McDowell, T.W. and Wu, J.Z. (2008), "A method for analyzing absorbed power distribution in the hand and arm substructures when operating vibrating tools", *J. Sound Vib.*, **311**(3), 1286-1304.
- Dong, R., Wu, J., McDowell, T., Welcome, D. and Schopper, A. (2005), "Distribution of mechanical impedance at the fingers and the palm of the human hand", *J. Biomech.*, **38**(5), 1165-1175.
- Dong, R.G., Welcome, D.E., McDowell, T.W., Wu, J.Z. and Schopper, A.W. (2006), "Frequency weighting derived from power absorption of fingers-hand-arm system under  $z$ -axis vibration", *J. Biomech.*, **39**(12), 2311-2324.
- Guo, J., Lee, K.M., Zhu, D., Yi, X. and Wang, Y. (2012), "Large-deformation analysis and experimental validation of a flexure-based mobile sensor node", *Mechatronics*, IEEE/ASME Transactions on **17**(4), 606-616.
- Hsu, Y., Chien, H., Lin, C., Liao, L., Chen, S. and Chang, P. (2008), "A capacitive low-g three-axis accelerometer", *Proceedings of the Electronic Materials and Packaging*, EMAP 2008, International Conference on, IEEE.
- <http://www.hse.gov.uk/VIBRATION/hav/hav.xls> - HSE hand-arm vibration exposure calculator
- Li, Y. and Chen, Y. (2013), "A review on recent development of vibration-based structural robust damage detection", *Struct. Eng. Mech.*, **45**(2), 159-168.
- Luque, A., Flores, G., Perdignes, F., Medina, D., García, J. and Quero, J. (2013), "Single axis accelerometer fabricated using printed circuit board techniques and laser ablation", *Sensor. Actuat. A - Phys.*, **192**, 119-123.
- Lynch, J., Partridge, A., Law, K., Kenny, T., Kiremidjian, A. and Carryer, E. (2003), "Design of piezoresistive MEMS-based accelerometer for integration with wireless sensing unit for structural monitoring", *J. Aerospace Eng.*, **16**(3), 108-114.
- Myung, H., Lee, S. and Lee, B.J. (2009), "Design of structural health monitoring robot using modified structured light", *IES J. Part A: Civil. Struct. Eng.*, **2**(3), 162-173.
- Myung, H., Lee, S. and Lee, B. (2011), "Paired structured light for structural health monitoring robot system", *Struct. Health Monit.*, **10**(1), 49-64.
- Ni, Y., Li, B., Lam, K., Zhu, D., Wang, Y., Lynch, J. and Law, K. (2011), "In-construction vibration monitoring of a super-tall structure using a long-range wireless sensing system", *Smart Struct. Syst.*, **7**(2), 83-102.
- Peterson, D., Brammer, A. and Cherniack, M. (2008), "Exposure monitoring system for day-long vibration and palm force measurements", *Int. J. Industrial Ergonom.*, **38**(9), 676-686.
- Rokkam, M., Chatni, M.R., ul Haque, A. De Carlo, A.R., Robinson, B.F. Irazoqui, P.P. and Porterfield, D.M. (2007), "High-density data acquisition system and signal preprocessor for interfacing with microelectromechanical system-based biosensor arrays", *Rev. Sci. Instrum.*, **78**(4), 044303.
- Wen, L., Wouters, K., Haspelslagh, L., Witvrouw, A. and Puers, R. (2011), "An in-plane SiGe differential capacitive accelerometer for above-IC integration", *J. Micromech. Microeng.*, **21**(7), 074011.

- Xiaohan, W. and Xilin, L. (1996), "Nonlinear finite element analysis of reinforced concrete slit shear wall under cyclic loading [J] ", *J. Tongji University* 2.
- Zhang, J. and Chen, J. (2008), "Tool condition monitoring in an end-milling operation based on the vibration signal collected through a microcontroller-based data acquisition system", *Int. J. Adv. Manuf. Tech.*, **39**(1-2), 118-128.
- Zheng, X.D., Jin, Z.H., Wang, Y.L., Lin, W.J. and Zhou, X.Q. (2009), "An in-plane low-noise accelerometer fabricated with an improved process flow", *J. Zhejiang Univ. Sci. A.*, **10**(10),1413-1420.